Submitted to
31st International Conference on High Energy Physics, ICHEP02, July 24, 2002, Amsterdam
Abstract: **1024**
Parallel Session **10**
www-h1.desy.de/h1/www/publications/conf/conf_list.html

Search for Single Top Quark Production in $e^{\pm}p$ collisions at HERA

H1 Collaboration

Abstract

A search for anomalous top quark production mediated by a flavour changing neutral current via a γ-u-t coupling is performed in $e^{\pm}p$ collisions at HERA. The search exploits data from an integrated luminosity of 115.2 pb^{-1}. The top decays into a b-jet and a W boson are considered in both the leptonic and the hadronic decay modes of the W. In the leptonic decay modes, five events are found to be compatible with the hypothesis of anomalous top quark production while 1.8 events are expected from the Standard Model. No excess above the Standard Model expectation is found in the hadronic decay channel. An upper limit on the anomalous γ-u-t coupling of $\kappa_{\gamma,u} = 0.22$ is established in the framework of recent NLO calculations.

1 Introduction

The H1 collaboration have reported [1] the observation of the production of events with energetic isolated leptons and missing transverse momentum in the positron-proton data collected in 1994-1997. Events with the same characteristics were also observed in the data collected from 1998-2000 [2]. In some of the events in both these data-sets, the hadronic final state is observed to have large transverse momentum. This is not typical for the primary Standard Model source of such events, namely the direct production of W bosons.

These outstanding events may indicate the presence of a further production mechanism involving processes beyond the Standard Model. One such mechanism is the production of top quarks which predominantly decay into a b-quark jet and a W boson. The lepton and the missing transverse momentum would then be associated with the leptonic decay of a W boson. Within the Standard Model, the rate of top quark production is negligible in $e^{\pm}p$ collisions at HERA energies. However, in several extensions of the Standard Model, the top quark is predicted to have significant flavour changing neutral current (FCNC) interactions, which could lead to a sizeable single top production cross-section at HERA.

In this paper we present a search for top quark production using the H1 detector at HERA. The analysis uses the data collected between 1994 and 2000 corresponding to an integrated luminosity of 115.2 pb^{-1}. Both the semileptonic decays and the hadronic decays of the top quark are investigated.

2 Phenomenology

Standard Model neutral current interactions preserve the involved flavours to leading order perturbation theory. Therefore, flavour changing neutral current (FCNC) processes only arise via higher order radiative corrections and are highly suppressed. Their low rate makes FCNC processes an ideal place to look for new physics at high energy colliders. Due to the large top quark mass, close to the electroweak symmetry breaking scale, deviations from the Standard Model might be observed first in the top sector. FCNC interactions involving the top quark have thus received considerable attention since the discovery of the top at the Fermilab TeVatron [3, 4]. Such interactions are present in many extensions of the Standard Model, which contain an extended Higgs sector [5], supersymmetry [6], dynamical breaking of the electroweak symmetry [7] or an additional symmetry [8].

At HERA, single top quark production is kinematically allowed due to the ep centre-of-mass energy of more that 300 GeV, well above the top quark mass. A FCNC vertex involving the coupling of the top quark to a light quark (u or c) and a gauge boson would lead to single top quark production, as illustrated in Fig. 1. The crossed process, $e^+e^- \rightarrow t\bar{q}(\bar{t}q)$, has been searched for at the LEP2 collider [9].

We consider here the most general effective Lagrangian, proposed in [10], which describes FCNC top quark interactions involving electroweak bosons:

$$\mathcal{L}_{eff} = \sum_{U=u,c} i\frac{ee_U}{\Lambda}\bar{t}\sigma_{\mu\nu}q^{\nu}\kappa_{\gamma,U}UA^{\mu} + \frac{g}{2\cos\theta_W}\bar{t}\left[\gamma_{\mu}(v_{Z,U} - a_{Z,U}\gamma^5) + i\frac{1}{\Lambda}\sigma_{\mu\nu}q^{\nu}K_{Z,U}\right]UZ^{\mu} \quad + \text{h.c.}, \tag{1}$$

where $\sigma_{\mu\nu} = (i/2)\,[\gamma^\mu, \gamma^\nu]$, θ_W is the Weinberg angle, q the four-momentum of the exchanged boson, e and g denote the gauge couplings relative to $U(1)$ and $SU(2)$ symmetries respectively, e_U denotes the electric charge of up-type quarks, A^μ and Z^μ the fields of the photon and Z boson, and Λ denotes the scale up to which the effective theory is assumed to hold. By convention we set $\Lambda = m_t$ in the following. Only magnetic operators allow FCNC $tq\gamma$ couplings, denoted by $\kappa_{\gamma,q}$, while q-t transitions involving the Z boson may also occur via vector interactions due to the non-vanishing Z mass. Single top production in ep collisions is, however, dominated by the t-channel exchange of a γ and therefore we concentrate here on the $\kappa_{\gamma,q}$ couplings.

The possibility of anomalous single top production at HERA was first investigated in [8] where a model was built in which $\kappa_{\gamma,q} \propto m_q^2$, and therefore only the $tc\gamma$ coupling was relevant. We do not rely here on any assumption concerning the underlying theory and thus allow both couplings $\kappa_{\gamma,c}$ and $\kappa_{\gamma,u}$ to be present and not necessarily related to each other. The sensivity of HERA is naturally much higher for the coupling $\kappa_{\gamma,u}$ than for $\kappa_{\gamma,c}$ as the u-quark density in the proton is larger than the c-quark density in the kinematic region at high Bjørken x, important for t-quark production. So far, the most stringent existing bound on $\kappa_{\gamma,u}$ comes from upper limits on radiative top decays set by the CDF Collaboration [11] : $BR(t \to u\gamma) < 3.2\%$ at 95% confidence level (CL), leading to $\kappa_{\gamma,u} < 0.42$ [10]. With this upper limit on $\kappa_{\gamma,u}$ the single top cross-section at HERA has been calculated to be ~ 1 pb, sufficiently large to allow several single top events to be produced with the current integrated luminosity.

The cross-section calculation for single top quark production has recently been improved by including next-to-leading order terms [12]. The correction increases the cross-section by roughly 20%, and is taken into account in the results derived in section 7.

3 Monte Carlo Event Generators

Events which are candidates for single top quark production are detected through semileptonic and hadronic decays of the top quark. The relevant final state topologies are an isolated lepton with high transverse momentum, a jet and missing transverse momentum for the semileptonic decay channel and three or more jets with high transverse momentum for the hadronic decay channel.

The simulation of the single top signal relies on the event generator ANOTOP which uses the matrix elements of the complete $e + q \to e + t \to e + b + W \to e + b + f + \bar{f}'$ process as obtained from the CompHEP [13] program. This allows a proper description of angular distributions. The BASES/SPRING [14] package is used to perform the numerical integration of the amplitudes and to generate events according to the differential cross-section. The parton shower approach [15] relying on the DGLAP [16] evolution equations is used to simulate QCD corrections in the initial and final states. The MRST LO parton densities are used for the proton [17]. The parton densities are evaluated at the top mass scale in analogy with the leptoproduction of heavy quarks.

The main Standard Model background contribution to the leptonic channel is the production of W bosons with the subsequent leptonic decay of the W [2]. Other processes with the same observed final state are lepton pair production and neutral current and charged current deep

inelastic scattering. In the hadronic channel, multi-jet electro- or photoproduction is the most important Standard Model background.

The production of the electroweak vector bosons Z^0 and $W^{\pm}$ is modelled using the EPVEC [18] event generator. Contributions from two-photon processes where one γ originates from the proton are calculated using the LPAIR [19] event generator.

To estimate the background contribution from neutral current (NC) or charged current (CC) deep inelastic scattering (DIS) for the leptonic decay channel of the top quark we use the DJANGO [20] event generator. DJANGO includes first order QED radiative corrections. The simulation of real bremsstrahlung photons, based on HERACLES [21], is also included. QCD radiation is treated following the approach of the Color Dipole Model [22], which simulates higher order effects, and is implemented using ARIADNE [23]. The hadronic final state is generated using the string fragmentation model [15]. In the hadronic decay channel of the top quark, the RAPGAP [24] event generator is used to study multi-jet production in NC DIS.

For direct and resolved photoproduction, we use the PYTHIA Monte Carlo event generator [25] which relies on first order QCD matrix element and uses leading-log parton showers and string fragmentation [15]. Both light and heavy flavours are generated. The GRV LO (GRV-G LO) parton densities [26] in the proton (photon) are used.

4 Experimental Conditions

The analysis is based on $e^{\pm}p$ collisions recorded by the H1 experiment in the 1994-2000 period. The data used were obtained during periods in which the central drift chambers, the liquid argon calorimeter and the luminosity system were active and fully operational.

The right handed cartesian coordinate system used in the following has its origin at the nominal primary interaction vertex. The proton direction defines the direction of the z axis and polar angles, θ, are defined with respect to this axis. The region with $\theta < 90^{\circ}$ is referred to as the "forward" region.

A detailed description of the H1 detector can be found in [27]. Components essential for this analysis are briefly described here. A tracking system consisting of central and forward drift chambers is used to measure the trajectories of charged particles and to determine the position of the interaction vertex. Particle transverse momenta are determined from the curvature of the trajectories in a magnetic field of 1.15 Tesla.

Surrounding the tracking system is a highly segmented calorimeter [28], which is 5 to 8 interaction lengths deep depending on the polar angle of the particle. The calorimeter is contained within a superconducting coil and an iron yoke instrumented with streamer tubes. Leakage of hadronic showers through the calorimeter is measured using the streamer tubes (Tail Catcher), as are the tracks of penetrating charged particles, such as muons, which are detected with an efficiency of above 90%.

The trigger condition for interactions leading to high transverse energy in the final state is based on calorimeter signals. The efficiency is larger than 95% for events with a scattered electron with an energy of at least 10 GeV, and larger than 85% for events with a calorimetric missing transverse momentum above 25 GeV. For multi-jet events the trigger efficiency is 100%.

5 Search for Single Top Quark Production in the Leptonic Decay Channel

The search for top quark decays in the leptonic decay channel is based on the selection of events with isolated leptons and missing transverse energy performed in [2]. The basic pre-selection criteria are the presence of a lepton with high transverse momentum $P_T^\ell > 10$ GeV and large missing transverse momentum above 12 GeV in the event. This serves to select events containing W bosons. In addition, the transverse momentum P_T^X of the hadronic final state X is required to be larger than 25 GeV. The W pre-selection is then further optimized to separate top production from Standard Model W production using the following top selection cuts:

- **Transverse momentum and polar angle of the jet**
  In top decays the hadronic system is expected to have a high transverse momentum. Energy deposits in the calorimeter and tracking information are used in an inclusive k_T algorithm [29, 30] to identify jets. The expected P_T distribution of the highest P_T jet is presented in the figure 2. It is shown in two angular domains. The highest P_T jet is required to have $P_T^{jet} > 25$ GeV. This threshold is set to 35 GeV if the jet has a polar angle of $\theta_{jet} < 35^\circ$.

- **Transverse mass of the lepton-neutrino system**
  This quantity is defined as the invariant mass of the two massless vectors obtained by projecting the lepton and neutrino momenta in the transverse plane, where the transverse neutrino momentum is calculated from the missing transverse momentum P_T^{miss} in the event:
  $$M_T^{\ell\nu} = \sqrt{\left(|\vec{P}_T^{\,\ell}| + |\vec{P}_T^{\,miss}|\right)^2 - \left(\vec{P}_T^{\,\ell} + \vec{P}_T^{\,miss}\right)^2}. \quad (2)$$
  For leptonic decays of the W, the most probable value of this quantity is close to the W mass and its distribution has a tail towards low masses. In order to reduce the contribution from processes with off-shell W bosons, a cut is applied on the transverse mass $M_T^{\ell\nu} > 10$ GeV.

- **Charge of the lepton**
  The production of top quarks in a γ-u fusion process yields t-quarks with charge $+2/3$. The corresponding charge conjugate $\bar{t}$ production in a γ-$\bar{u}$ fusion process involving sea quarks is suppressed by a factor of ~ 80. It is not covered in this analysis. The decay $t \to bW^+(\to \ell^+\bar{\nu})$ produces only positively charged isolated leptons. To reduce contributions from processes other than top quark production to the selected event sample, leptons for which the charge measurement yields the wrong sign with a precision better than 2σ are rejected.

  The reliability of the charge measurement at high P_T has been tested using a sample of neutral current events collected in e^+p collisons. The scattered electrons are required to have a transverse momentum above 20 GeV, measured from calorimeter deposits, and a corresponding track transverse momentum above 10 GeV. The track corresponding to the scattered electron has to be isolated and must have a charge measurement from curvature with a precision of at least two standard deviations. The wrong sign assignment rate is

below 1% in this sample. In a sub-sample of forward electrons with polar angle $\theta < 50^{\circ}$, where most of the signal is expected, the wrong charge assignment has been determined in the data to be less than 2%.

The total numbers of selected events are presented in the tables 1 and 2 for an analysed data sample corresponding to 101.6 pb^{-1} in e^+p collisons and 13.6 pb^{-1} in e^-p collisions. In the e^+p data 4 events containing electrons and 6 events containing muons are observed at $P_T^X > 25$ GeV [2]. After the full top selection described above, 3 electron events and 2 muon events remain as top candidates for a Standard Model background estimation of 0.75 ± 0.18 (e^+p) plus 0.13 ± 0.04 (e^-p) for the electron channel and 0.77 ± 0.21 (e^+p) plus 0.12 ± 0.03 (e^-p) for the muon channel.

	W pre-selection		Top selection	
	Electron Channel	Muon Channel	Electron Channel	Muon Channel
Data	4	6	3	2
Standard Model	1.29 ± 0.33	1.54 ± 0.41	0.75 ± 0.18	0.77 ± 0.21
W only	1.05 ± 0.32	1.29 ± 0.39	0.51 ± 0.16	0.68 ± 0.19
Top efficiency	43%	51%	37%	45%

Table 1: Observed and predicted number of events for the W pre-selection cuts and the top selection cuts in e^+p data corresponding to 101.6 pb^{-1}

	W pre-selection		Top selection	
	Electron Channel	Muon Channel	Electron Channel	Muon Channel
Data	0	0	0	0
Standard Model	0.26 ± 0.06	0.20 ± 0.07	0.13 ± 0.04	0.12 ± 0.03
W only	0.16 ± 0.05	0.18 ± 0.06	0.07 ± 0.02	0.10 ± 0.03
Top efficiency	43%	51%	37%	45%

Table 2: Observed and predicted number of events for the W pre-selection cuts and the top selection cuts in e^-p data corresponding to 13.6 pb^{-1}

In order to calculate the invariant masses of the lepton-neutrino system and the system consisting of the lepton, the neutrino, and the hadronic final state, the event kinematics has to be reconstructed. The following variables are used to quantify the kinematics:

- $\vec{P}_T^{\ell}$: Transverse momentum vector of the isolated lepton. The calculation of the transverse momentum is performed using calorimetric information for electrons and central tracker information for muons.
- E^{ℓ}: Energy of the isolated lepton.
- $\vec{P}_T^{X}$: Transverse momentum vector of the hadronic system. This is calculated as the vector sum of all energy deposits in the liquid argon calorimeter and the tail catcher calorimeter not including energy deposited by any additional leptons.

- E^X: Energy of the hadronic system.
- $\vec{P}_T^{miss}$: Total missing transverse momentum vector of the event. This is defined as the vector sum of the transverse momenta of all final state particles: $\vec{P}_T^{miss} = -(\vec{P}_T^{lepton(s)} + \vec{P}_T^X)$. The missing transverse momentum is attributed to the hypothetical neutrino.
- δ^{vis}: Total visible longitudinal momentum balance, defined as the scalar sum of $(E - P_z)$ over all final state particles: $\delta^{vis} = (E - P_z)^{lepton(s)} + (E - P_z)^X$
- $M_T^{\ell\nu}$: Transverse mass of the lepton-neutrino system defined in equation 2.

To compute the complete event kinematics the neutrino four-vector needs to be reconstructed. The transverse momentum of the neutrino corresponds to the total missing transverse momentum $\vec{P}_T^{miss}$ of the event. As regards the longitudinal momentum of the neutrino, two cases are treated separately:

- *Tagged events:* In this case the scattered electron is detected in one of the calorimeters. In the muon channel this means that the event contains an identified electron and in the electron channel the event contains an additional electron of lower transverse momentum. We assume that the electron with the lowest transverse momentum is the scattered electron (which is the correct choice in 95% of top events according to the simulation.) For tagged events, the invariant mass of the lepton-neutrino-hadron system is computed using the neutrino kinematics deduced from longitudinal energy conservation. We obtain $(E - P_z)^\nu = 55$ GeV $-\delta^{vis}$ using the longitudinal momentum balance defined above. For two events of the ten with $P_T^X > 25$ GeV given in table 1 this method can be applied.
- *Untagged events* The scattered electron is not detected and therefore its longitudinal momentum is unknown. We therefore apply a constraint on the invariant mass of the lepton and the neutrino from the W decay:

$$M_{\ell\nu} = \sqrt{P_\ell^2 + P_\nu^2 + 2P_\ell P_\nu} \approx \sqrt{2P_\ell P_\nu} = M_W = 80.2\,\text{GeV} \tag{3}$$

  where P_ℓ and P_ν denote the four-vectors of the lepton and neutrino, respectively. This constraint on the W mass yields two possible solutions for $(E - P_z)^\nu$, one corresponding to a backward neutrino (solution 1), the other to a forward neutrino (solution 2) relative to the lepton direction. For both possible solutions for the neutrino, the invariant mass of the lepton-neutrino-hadrons system $M_{\ell\nu X}$ can be calculated. Solutions that fail any of the following requirements are rejected as being unphysical:

  - $M_{\ell\nu X} < \sqrt{s}$ where $\sqrt{s}$ is the electron-proton cms energy (300 GeV or 320 GeV depending on data taking period).
  - 0 GeV $< (E - P_z)^\nu < 55$ GeV
  - $(E - P_z)^\nu + \delta^{vis} < 75$ GeV
  - $E^\nu + E^X + E^{lepton(s)} < 1000$ GeV

The requirements ensuring energy and $E - P_z$ conservation were optimized on a sample of generated top events in order to leave some scope for fluctuations in the energy measurement.
If no solution exists, the measurement errors on the energy of the hadronic final state E^X (electron channel) or the transverse momentum of the muon P_T^μ (muon channel) are taken into account as these are the dominant errors in those channels. New masses are computed using values of E^X or P_T^μ varied by $\pm 1\sigma$. If a solution is still not found then a $\pm 2\sigma$ variation is performed. The solution yielding the lowest mass is chosen as a lower 1σ or 2σ limit.

A study using events generated with the ANOTOP Monte Carlo showed that this mass reconstruction procedure has an 80% reconstruction efficiency in the electron channel and a 65% efficiency in the muon channel. In figure 3 distributions of the reconstructed top mass are shown for ANOTOP Monte Carlo events in both the electron and the muon channels. The widths of the mass distributions are determined to $\sigma(M_{top}) = 20$ GeV for electrons and $\sigma(M_{top}) = 22$ GeV for muons.

The mass solutions obtained for the isolated lepton events in the W pre-selection can be found in table 3. Two events (one electron and one muon event) contain the scattered electron and therefore the "tagged" method can be applied. As a check it can be seen that for the two tagged events the masses reconstructed with the "tagged" and one of the solutions of the "untagged" method are compatible. In the top selection as defined above, the first three of the four observed electron events and the two last muon events in table 3 are selected as top candidates. One electron and one muon event do not fulfill the P_T^{jet} requirement. One muon event does not pass the cut on $M_T^{\ell\nu}$, and the remaining two muon events are not selected as top candidates because of their negative charge.

		Untagged Solution 1		Untagged Solution 2		Tagged Solution
	PT(X) (GeV)	Mass (GeV)	$E - P_z$ (GeV)	Mass (GeV)	$E - P_z$ (GeV)	Mass (GeV)
e^+ top cand.	41	159 ± 7	61	136 ± 6	21	–
e^+ top cand.	43	–	–	166 ± 8	54	165 ± 6
e^+ top cand.	39	178 ± 5	39	156 ± 7	21	–
e^+	27	234 ± 15	65	199 ± 14	38	–
μ^+	42	–	–	146 ± 7	19	–
μ^-	27	152 ± 12	53	129 ± 6	34	156 ± 10
$\mu^-(1\sigma)$	59	180	67	188	37	–
$\mu\ (2\sigma)$	30	157	53	139	22	–
μ^+ top cand.	67	–	–	181 ± 10	19	–
μ^+ top cand.	50	–	–	174 ± 12	39	–

Table 3: $M_{\ell\nu X}$ calculation for the ten events in the W pre-selection. Untagged solutions (mass and total $E - P_z$) using a W constraint are presented for all events. In two events the scattered electron is detected and the tagged mass solution using an $E - P_z$ constraint can be obtained. The events selected as top candidates are indicated.

The total lepton-neutrino-hadrons mass distributions of the final top candidates are compared to the Standard Model prediction in figure 4.

6 Search for Single Top Quark Production in the Hadronic Decay Channel

A search for the production of top quarks is also performed in the hadronic decay channel. The decay cascade $t \to bW(\to q\bar{q})$ yields events with at least three jets with high transverse momenta P_T. The main Standard Model background is the electro- or photoproduction of high P_T jets.

6.1 3-Jet Pre-Selection

The search for 3-jet events is performed using an inclusive k_T algorithm [29, 30] based on calorimetric energy deposits combined with well-measured tracks of transverse momentum below 2 GeV. Only jets in the pseudorapidity range $-0.5 < \eta_{jet} < 2.5$ and with transverse momenta $P_T > 4$ GeV are considered. In order to remove mis-identified electrons, each jet is required to have either an electromagnetic energy fraction of less than 90% or a size in the η-ϕ plane larger than 0.1. These criteria define the hadronic jets in each event. Events with at least three hadronic jets fulfilling $P_T^{Jet1} > 25$ GeV, $P_T^{Jet2} > 20$ GeV and $P_T^{Jet3} > 15$ GeV are selected. These criteria define the 3-jet pre-selection in the following.

The photoproduction regime $Q^2 < 4$ GeV^2 is modelled using the PYTHIA generator. Neutral Current DIS processes with $Q^2 > 4$ GeV^2 are simulated with RAPGAP [24]. An overall normalization factor of 1.25 is required to fit the measured electro- and photoproduction cross-sections and is applied to the rate predicted by PYTHIA for $Q^2 < 4$ GeV^2 and RAPGAP for $Q^2 > 4$ GeV^2.

In figure 5 distributions of various kinematic quantities are shown for the events in the 3-jet pre-selection together with the Standard Model expectation. The transverse momenta of the jets, the invariant mass of all jets M_{jets}, the total transverse momentum $E_{T,tot}$ (defined as the scalar sum of the transverse momenta of all hadronic jets with $P_T^{jet} > 4$ GeV), and the total $E - P_z$ are all observed to be well described by the Standard Model prediction.

6.2 High E_T 3-Jet Selection and Discriminating Observables

To enhance the top signal relative to the background the phase space is further restricted to the high transverse momentum region with $P_T^{Jet1} > 40$ GeV, $P_T^{Jet2} > 25$ GeV and $P_T^{Jet3} > 20$ GeV. In addition a total amount of hadronic transverse energy $E_{T,tot} > 110$ GeV is required in each event. These harsher selection criteria are referred to as the high E_T 3-jet selection.

Top induced events are expected to have a 2- and 3-jet invariant mass close to the W and top mass, respectively. In order to exploit the different invariant mass combinations of the jets and the angular decay properties of the top quark to discriminate the top signal from the QCD background, the events are decomposed as follows. The three highest P_T jets are associated to the hadronic decay of the W and to the b-jet according to the following procedure:

- The two jets having an invariant mass closest to the W boson mass are assigned to the W decay products.
- The remaining jet among the three highest P_T jets is assigned to the b-jet from the top decay.

A study using the ANOTOP Monte Carlo generator showed that this hypothesis identifies the correct b-jet in $\approx 70\%$ of the events. Good discrimination between top production and QCD background is provided by the angle between the two jets from the W decay in the top rest frame, denoted by the angle θ^* in the following. This angle tends to be close to 180° for QCD background, where a dijet mass close to the W mass is achieved by picking a back-to-back dijet pair in the top rest frame. In contrast, for top decays, the angle θ^* typically has values close to 140° due to the boost of the W decay products in the top rest frame. The distribution of $\cos\theta^*$ is shown in figures 6 and 7 together with the other observables used to discriminate the top signal from the Standard Model background.

To select top candidates in the data sample defined above, the invariant dijet mass closest to the mass of the W boson has to fulfill $70 < M^{2jet}_{Wcomb.} < 90$ GeV, and the invariant mass of all jets has to be reconstructed in a window around the top mass given by $150 < M_{jets} < 210$ GeV. In addition it is required that $\cos\theta^* > -0.5$. The top selection cuts are summarized in table 4. For this selection the efficiency is estimated with the Monte Carlo model ANOTOP to be 27%. After applying the top selection criteria, 14 candidate events are selected compared to 19.6 ± 7.8 events expected from the Standard Model processes as seen in table 5.

	Top selection cut
W mass window	70 GeV $< M^{2jet}_{Wcomb.} < 90$ GeV
Top mass window	150 GeV $< M_{jets} < 210$ GeV
Decay angle θ^*	cos $\theta^* > -0.5$

Table 4: Summary of the top selection cuts in the hadronic decay channel.

The main experimental systematic errors in this analysis are due to the uncertainty in the absolute hadronic energy calibration of the calorimeter and the measurement of the polar angles of the jets. Systematic effects due to the uncertainty in the luminosity measurement and trigger inefficiencies are negligible. The theoretical error we assign to the Standard Model expectation in the signal region is 30%. This is estimated from the comparison of the total transverse momentum distributions of the data and the Monte Carlo simulation for the high E_T 3-jet selection. At highest $E_{T,tot}$, where the top signal is expected, agreement is seen at the 30% level. The total systematic error in the hadronic decay channel amounts to 40%. Figure 8 shows the invariant mass M_{jets} of the top candidates together with the Standard Model prediction.

7 Results

We first consider the hadronic decay channel of the top quark. Here no deviation from the Standard Model prediction is observed, as reported in section 6. Assuming Poisson distributions for

	Top selection cuts
Data	14
Standard Model	19.6 ± 7.8
Efficiency ($t \to 3$ jets)	27%

Table 5: Number of observed and expected events in the top selection for the hadronic decay channel in the 1994-2000 data.

the Standard Model background and for the top signal, an upper limit at 95% confidence level (CL) on the number of events coming from singly produced top quarks decaying hadronically is obtained using a standard Bayesian prescription. This limit is then converted into an upper limit on the top production cross-section at $\sqrt{s} = 320$ GeV by folding in the corresponding efficiency and branching ratio. The branching $t \to bW$ is assumed to be 100%, which is a safe approximation as seen from the CDF upper bound on radiative top decays into $q\gamma$ [11]. This results in an upper bound $\sigma_{320} = \sigma(ep \to etX, \sqrt{s} = 320 \text{ GeV}) < 0.40$ pb.

With the upper bound derived from the hadronic channel, we calculate upper limits on the number of semileptonic top quark decays and compare them to the number of observed lepton events. At 95% CL, less than 1.3 (4.1) events coming from single top production should be observed with our selection criteria in the electronic and muonic decay channels in the e^+p data taken at $\sqrt{s} = 300$ GeV ($\sqrt{s} = 320$ GeV), while 1 (4) candidate(s) is (are) observed. The upper limit derived from the hadronic decay channel therefore does not rule out an interpretation of the observed events in the leptonic channel as anomalous top production.

The number of observed and expected events in the different channels for the e^+p and e^-p data are combined to set an upper bound on $\sigma(ep \to etX)$ at a given centre-of-mass energy, which is then translated into constraints on the anomalous coupling $\kappa_{\gamma,u}$. Each channel contributes in the derivation of the limits via its branching ratio, the number of observed and expected events satisfying the top selection cuts and the corresponding selection efficiencies. The three considered datasets (e^+p at $\sqrt{s} = 300$ GeV, e^-p at $\sqrt{s} = 320$ GeV, e^+p at $\sqrt{s} = 320$ GeV) are treated as independent channels, weighted by their relative luminosities and the ratio of the single top cross-section for the corresponding centre-of-mass energy to σ_{320}. The resulting upper limit, N_{lim}, on the number of signal events translates into an upper bound on the cross-section σ_{320} via $N_{\text{lim}} = \mathcal{L}_{tot} \times \sigma_{320}$. Both systematic and statistical errors have been folded in channel by channel as described in [31].

The resulting upper bound on the single top cross-section at $\sqrt{s} = 320$ GeV is :

$$\sigma(ep \to e + t + X, \sqrt{s} = 320 \text{ GeV}) < 0.43 \text{ pb} \qquad \text{at } 95\% \text{ CL} \quad .$$

This procedure results in an upper limit on the anomalous $tu\gamma$ magnetic coupling of :

$$\kappa_{\gamma,u} < 0.22.$$

The obtained HERA limit improves the CDF upper bound coming from radiative top decays by about a factor of two. Single top searches at LEP2 have also been formulated in terms of bounds on the anomalous couplings. Since e^+e^- collisions also provide sensitivity to anomalous tqZ couplings, the couplings κ_γ and v_Z have been considered simultaneously. The preliminary

results obtained by LEP [9], using data with $\sqrt{s}$ up to 209 GeV, are shown in Fig. 9, which represents the current status of the constraints on κ_γ and v_Z. The sensitivity of the HERA and TeVatron colliders to FCNC processes will significantly increase [32] with the large luminosities expected in the near future.

8 Summary

Events containing an isolated lepton with large transverse momentum, missing transverse momentum and a jet carrying large transverse momentum have been observed by the H1 Collaboration in data collected in both the 1994-1997 and 1998-2000 running periods. The missing transverse momentum and the leptons seen in these events are likely to result from W decay, but the rate at which they are observed is somewhat higher than expected in the Standard Model. This, together with the observed high transverse momentum hadron production, motivated the search for single top quark production described here.

Five isolated lepton events were selected as candidate single top events by this dedicated search in data samples corresponding to 101.6 pb^{-1} and 13.6 pb^{-1} in e^+p and e^-p collisions, respectively. The Standard Model prediction for this data sample is 1.77 $\pm$ 0.46 events.

The analysis of n-jet production ($n \geq 3$) shows no excess above the Standard Model expectation within the experimental and theoretical uncertainties. However, the limit on top production derived from the hadronic decay channel has insufficient sensitivity to rule out the single top interpretation for the candidates observed in the leptonic decay channels.

Assuming that the observed data contain only Standard Model processes, the lepton and n-jet events are used to derive an upper limit on the $t \leftrightarrow u$ transition mediated by a coupling to the photon. This bound extends into a region of parameter space not excluded by other experiments at LEP and the TeVatron.

Acknowledgements

We are grateful to the HERA machine group whose outstanding efforts have made and continue to make this experiment possible. We thank the engineers and technicians for their work in constructing and now maintaining the H1 detector, our funding agencies for financial support, the DESY technical staff for continual assistance, and the DESY directorate for the hospitality which they extend to the non-DESY members of the collaboration. We thank A.S. Belyaev for useful discussions and fruitful collaboration.

References

[1] C.Adloff *et al.* (H1 Collaboration), Eur. Phys. J. C5 3 (1998), 439.

[2] H1 Collaboration, "Isolated lepton events and W production ", contributed paper 802, EPS2001, Budapest.

[3] CDF Collaboration, Phys. Rev. Lett. 74 (1995) 2626.

[4] D0 Collaboration, Phys. Rev. Lett. 74 (1995) 2632.

[5] D. Atwood, L. Reina and A. Soni, Phys. Rev. D53 (1996) 1199.

[6] G.M. Divitiis, R. Petronzio and L. Silvestrini, Nucl. Phys. B504 (1997) 45.

[7] R.D. Peccei and X. Zhangh, Nucl. Phys. B337 (1990) 269.

[8] H. Fritzsch and D. Holtmannspötter, Phys. Lett. B457 (1999) 1199.

[9] ALEPH, DELPHI, L3, OPAL and the LEP EXOTICA working group, contributed paper submitted to Summer 2001 Conferences, LEP Exotica WG 2001-01, ALEPH 2001-055 CONF 2001-035, DELPHI 2001-119 CONF542, L3 Note 2706, OPAL TN698.

[10] T. Han and J.L. Hewett, Phys. Rev. D60 (1999) 074015.

[11] CDF Collaboration, F. Abe *et al.*, Phys. Rev. Lett. 80 (1998) 2525.

[12] A. Belyaev and N. Kidonakis, FSU-HEP-20010205, Feb 2001. 6pp (hep-ph/0102072).

[13] E.E. Boos *et al.*, SNUTP-94-116, hep-ph/9503280; E.E. Boos *et al.*, Proceedings of the Xth Int. Workshop on High Energy Physics and Quantum Field Theory, QFTHEP-95, (Moscow, 1995), Eds. B. Levtchenko and V. Savrin, p 101.

[14] S. Kawabata, Comp. Phys. Comm. 41 (1986) 127.

[15] JETSET 7.4; T. Sjöstrand, Lund Univ. preprint LU-TP-95-20 (August 1995) 321pp; *idem*, CERN preprint TH-7112-93 (February 1994) 305pp.

[16] V.N. Gribov and L.N. Lipatov, Sov. Journ. Nucl. Phys. 15 (1972) 78;
G. Altarelli and G. Parisi, Nucl. Phys. B126 (1977) 298;
Y.L. Dokshitzer, JETP 46 (1977) 641.

[17] A.D. Martin, R.G. Roberts, W.J. Stirling and R.S. Thorne, Euro. Phys. J. C4 (1998) 463.

[18] H1 generator based on EPVEC 1.0; U. Baur, J.A.M. Vermaseren and D. Zeppenfeld, Nucl. Phys. B375 (1992) 3.

[19] S. Baranov *et al.*, Proc. of the Workshop Physics at HERA, W. Buchmüller and G. Ingelman (Editors), (October 1991, DESY-Hamburg) Vol. 3, p. 1478; J.A.M. Vermaseren, Nucl. Phys. B229 (1983) 347.

[20] DJANGO 2.1; G.A. Schuler and H. Spiesberger, Proceedings of the Workshop Physics at HERA, W. Buchmüller and G. Ingelman (Editors), (October 1991, DESY-Hamburg), vol. 3 p. 1419.

[21] HERACLES 4.4; A. Kwiatkowski, H. Spiesberger and H.-J. Möhring, Comput. Phys. Commun. 69 (1992) 155.

[22] G. Gustafson and U. Pettersson, Nucl. Phys. B306 (1988) 746; *idem*, *addendum* Lund University preprint LU-TP-87-19, (October 1987) 4pp.; B. Andersson *et al.*, Z. Phys. C43 (1989) 625.

[23] ARIADNE 4.0; L. Lönnblad, Comput. Phys. Commun. 71 (1992) 15.

[24] H. Jung, Comp. Phys. Comm. **86** (1995) 147;
RAPGAP program mannual (1998) unpublished.

[25] PYTHIA 5.7; T. Sjöstrand, CERN-TH-6488 (1992), Comp. Phys. Comm. 82 (1994) 74.

[26] M.Glück, E.Reya and A Vogt, Phys. Rev. D45 (1992)3986; *idem*, Phys. Rev. D46(1992) 1973.

[27] H1 Collaboration, I. Abt et al., Nucl. Instr. and Meth. A386 (1997) 310 and 348.

[28] H1 Calorimeter Group, B. Andrieu et al., Nucl. Instr. and Meth. A336 (1993) 460.

[29] S. Catani, Y. L. Dokshitzer, M. H. Seymour and B. R. Webber, Nucl. Phys. B **406** (1993) 187.

[30] S. D. Ellis and D. E. Soper, Phys. Rev. **D48** (1993) 3160.

[31] H1 Collaboration, T. Ahmed *et al.*, Z. Phys. C64 (1994) 545.

[32] A. Belyaev, CERN-TH-2000-191, Jun 2000. 4pp (hep-ph/0007058), to be published in the Proceedings of the 8th International Workshop on Deep Inelastic Scattering and QCD (DIS 2000).

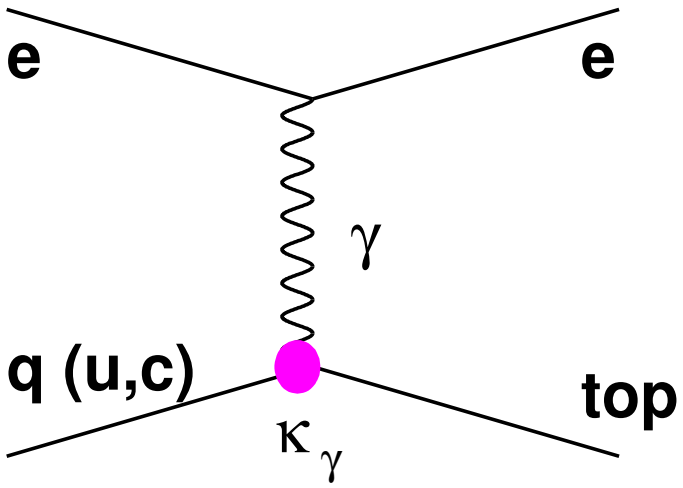

Figure 1: A Feynman diagram for anomalous single top production via a flavour changing neutral current interaction at HERA.

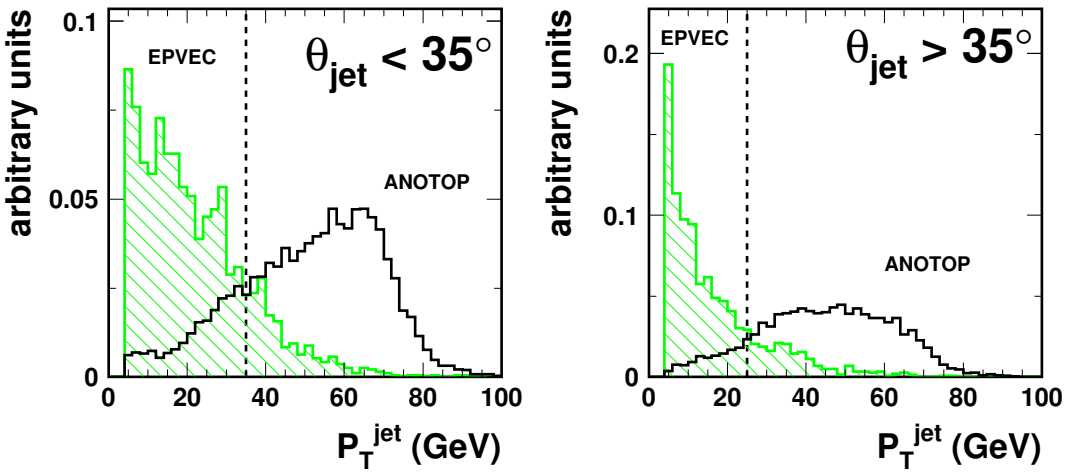

Figure 2: Expected distribution of the hadronic jet transverse momenta for W- production (shaded) and top production (open) in two regions of the jet polar angle. The values of the cuts applied in the analysis are indicated.

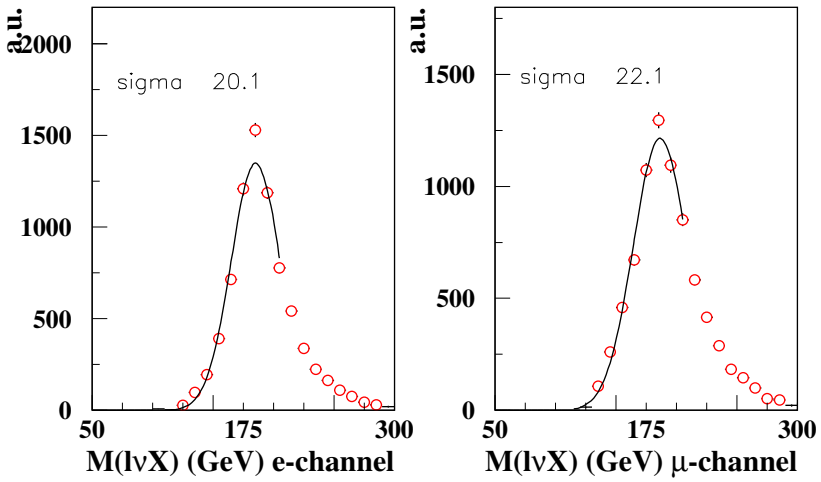

Figure 3: Reconstructed top mass as invariant mass of lepton, neutrino and hadrons in the electron channel (left) and muon channel (right). The mass resolutions are taken from gaussian fits to the mass distributions (solid line).

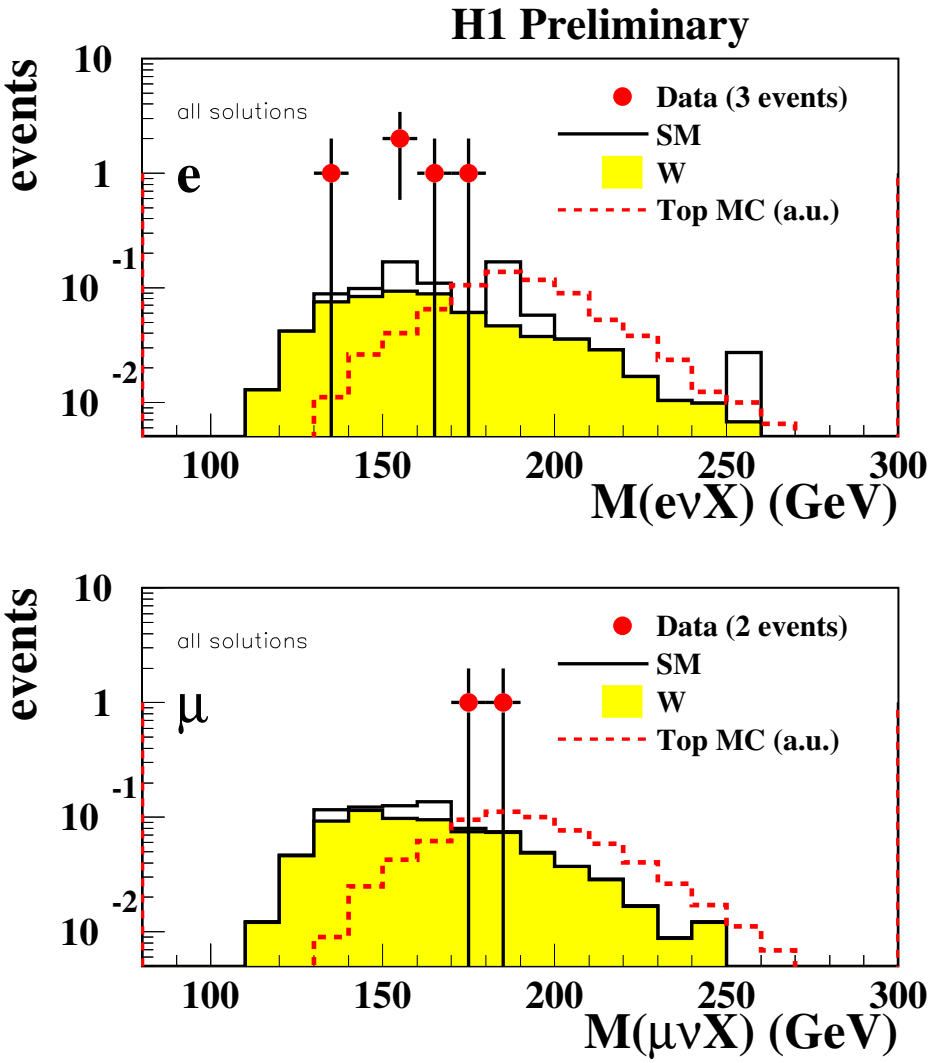

Figure 4: Distribution of the lepton-neutrino-hadrons mass for the top candidates (symbols) and the Standard Model expectation (white histogram). The shaded histogram represents the Standard Model W contribution. The dashed histogram represents the ANOTOP prediction for a rate corresponding to one event. All the solutions obtained by the procedure described in the text are displayed. In the data there are 3 electron candidates with 5 possible solutions and 2 muon candidates with 2 solutions. The precision of the individual mass measurements is better than 9 GeV for the electron candidates and better that 13 GeV for the muon candidates.

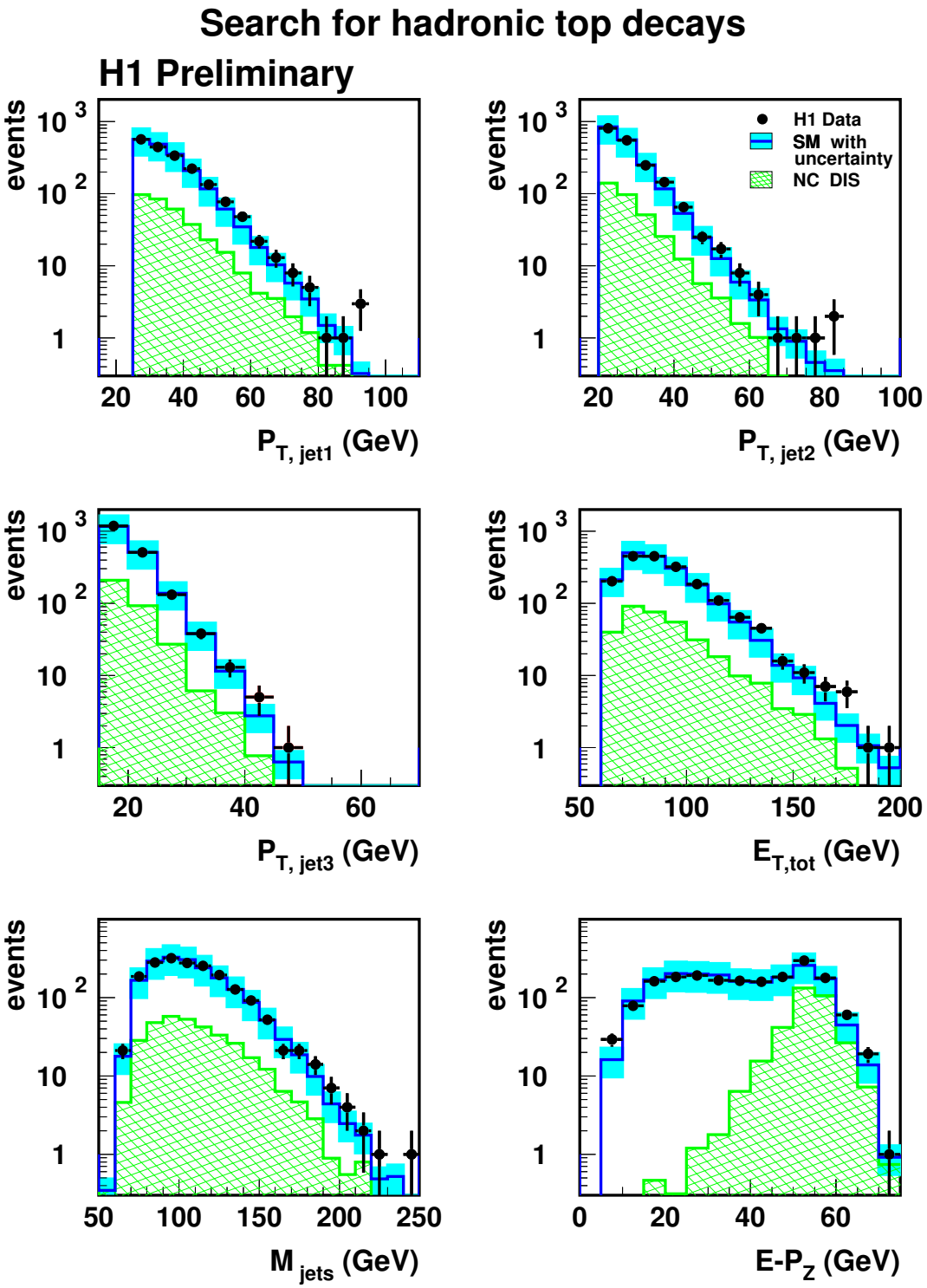

Figure 5: Distributions of jet transverse momentum for jets 1, 2 and 3, with $P_{T,jet} > 25, 20$ and 15 GeV (3-jet pre-selection), of the total transverse energy, $E_{T,tot}$, of the jet invariant mass M_{jets} and of the longitudinal energy-momentum balance $E - P_z$ for the data taken in the years 1994 to 2000.

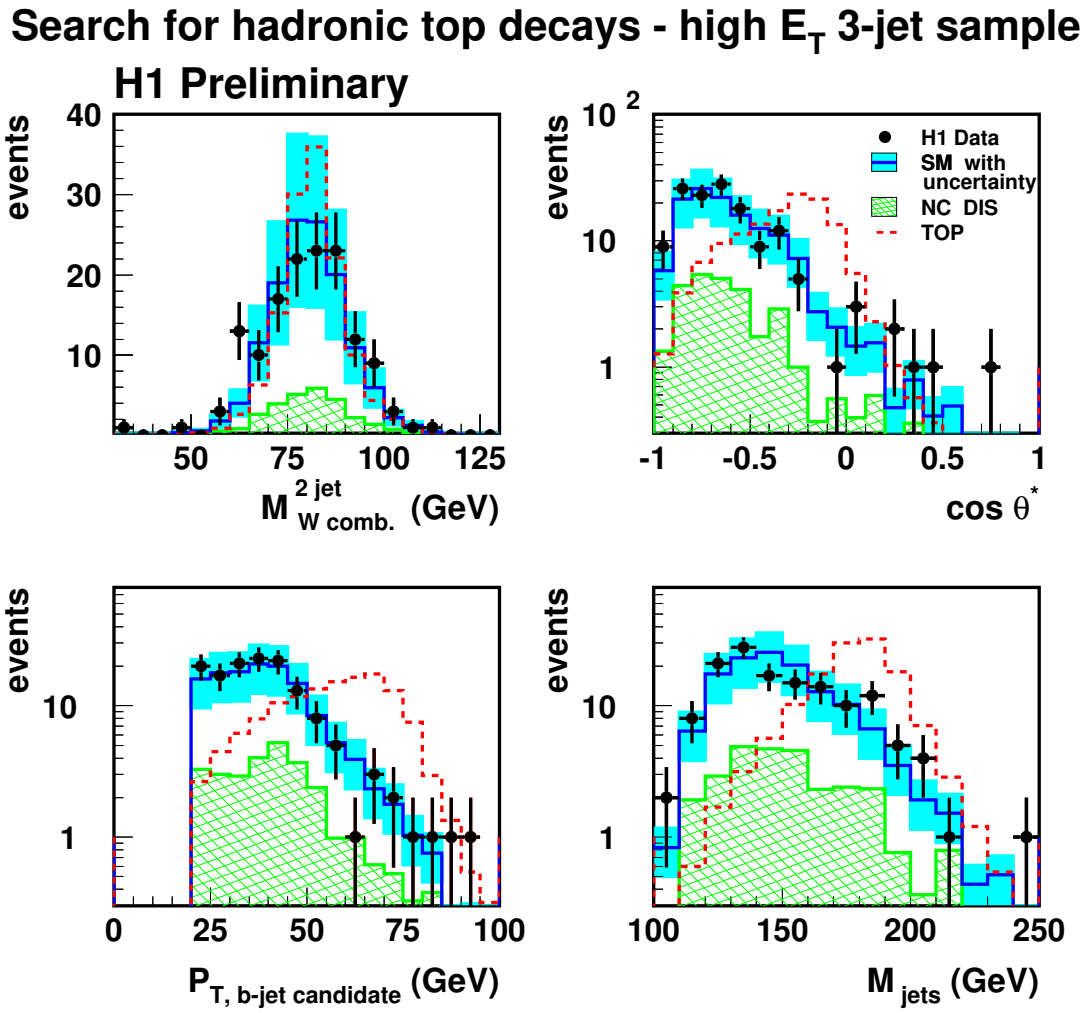

Figure 6: Observables used to discriminate top quark production from Standard Model processes in the high E_T 3-jet sample ($E_{T,tot} > 110$ GeV, $P_T^{jet} > 40, 25, 20$ GeV). The two jets with an invariant mass closest to 80 GeV are assigned to the W decay and the remaining high-P_T jet to the b-quark. The angle $\theta^\star$ denotes the angle in the top rest frame between the two jets from the W decay. The calculations of the ANOTOP Monte Carlo generator are displayed with arbitrary normalization.

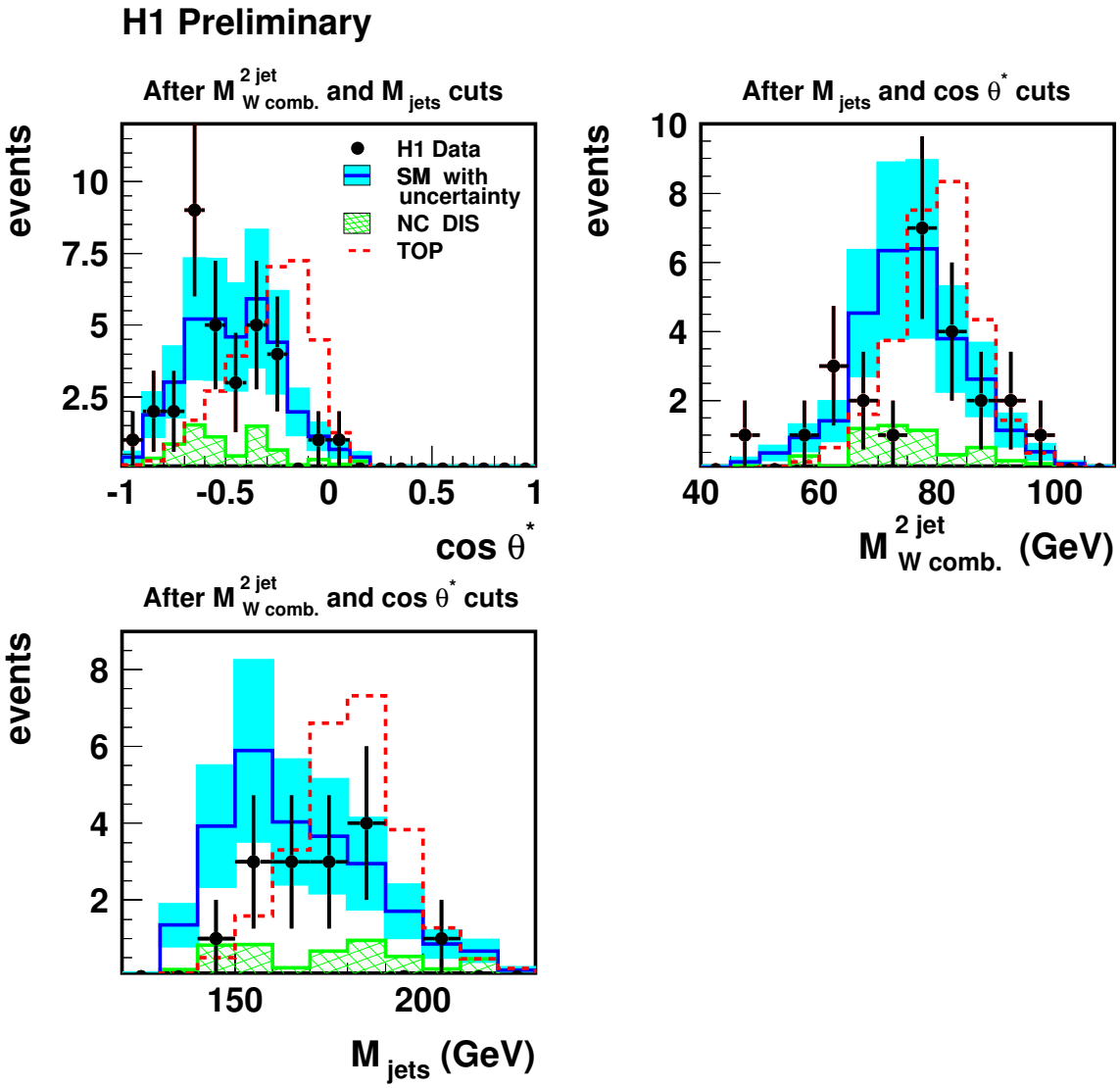

Figure 7: Distributions of the cosine of the decay angle $\theta^\star$ (which denotes the angle between the two jets from the W decay in the top rest frame), the invariant 2-jet mass of the two jets assigned to the W decay, and the invariant mass of all jets for the high E_T 3-jet selection. Each observable is shown after applying the top selection cuts (see table 4) on the other two discriminating observables.

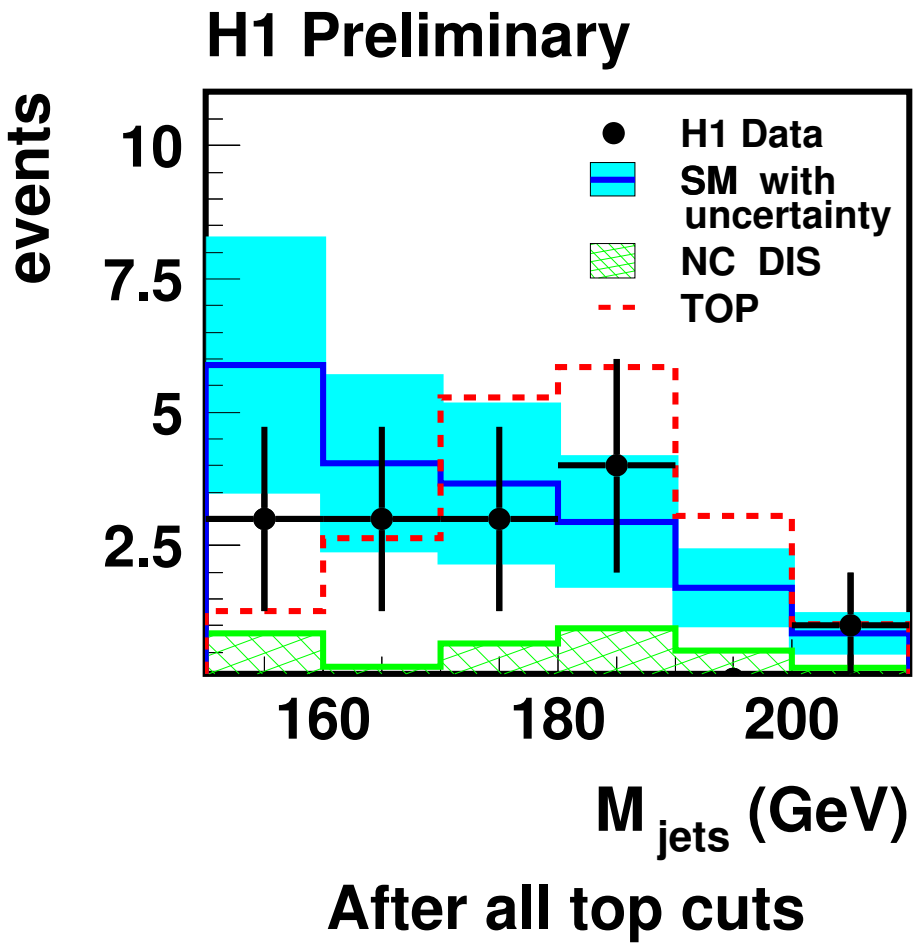

Figure 8: Reconstructed mass M_{jets} of the candidate events and the Standard Model expectation after all top selection cuts (see table 4). The calculations of the ANOTOP Monte Carlo generator are displayed with arbitrary normalization.

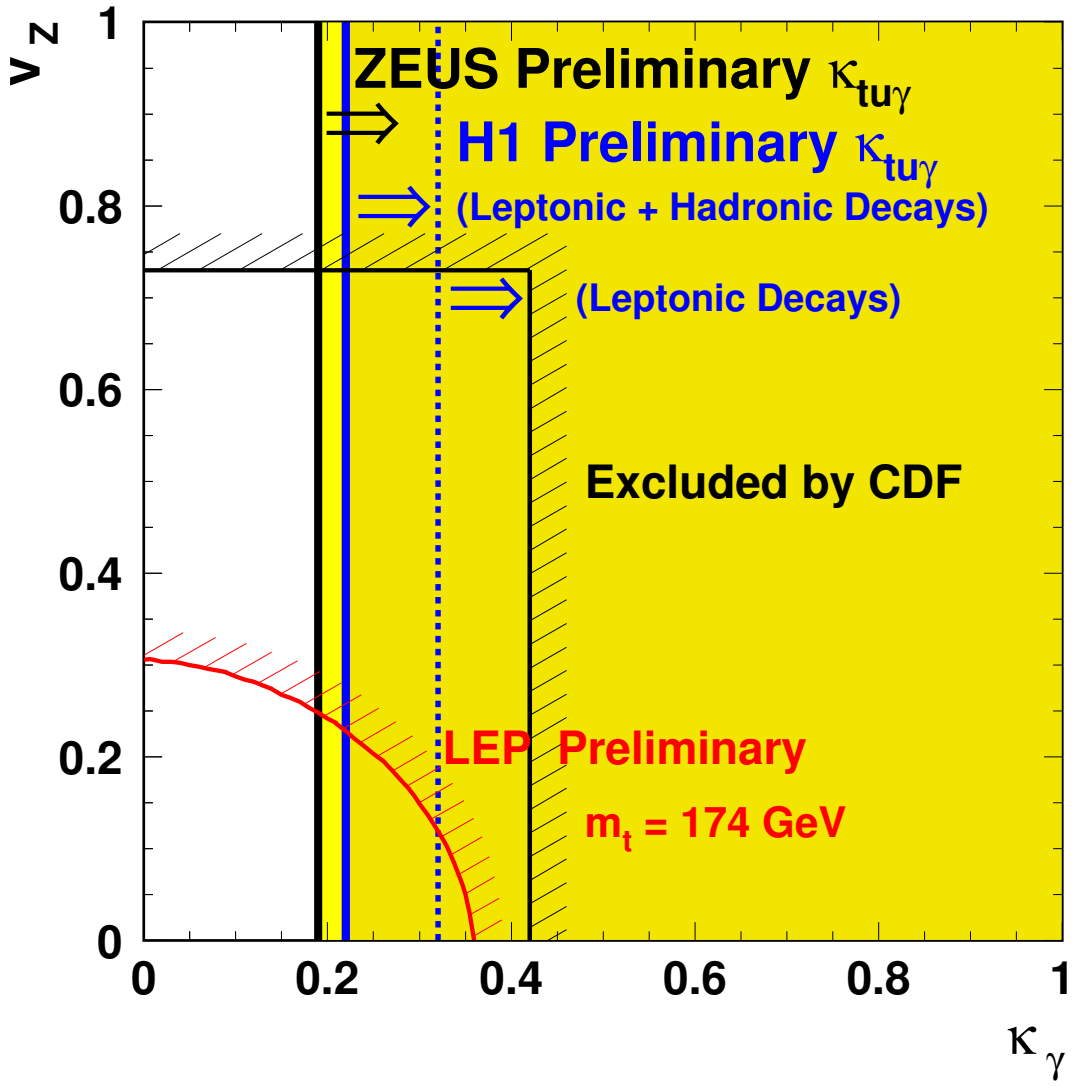

Figure 9: Exclusion limits at 95% CL on the anomalous $tq\gamma$ magnetic coupling κ_γ and the vector coupling v_Z obtained at the TeVatron, LEP and HERA colliders. The H1 limit applies to the coupling $\kappa_{\gamma,u}$ to the u-quark only. Both the H1 limit for leptonic decays and the H1 combined limit for leptonic and hadronic decays of the top quark are indicated.